2696 *Chem. Mater.* **2010,** *22,* 2696–2698
DOI:10.1021/cm100417z

CHEMISTRY OF
MATERIALS
Communication

Efficient Polymer Solar Cells Based on the Copolymers of Benzodithiophene and Thienopyrroledione

Yong Zhang, Steven K. Hau, Hin-Lap Yip, Ying Sun, Orb Acton, and Alex K.-Y. Jen*

Department of Materials Science and Engineering, University of Washington, Seattle, Washington 98195

Received February 9, 2010
Revised Manuscript Received March 30, 2010

Polymer solar cells (PSCs) have been recently vigorously explored as a promising renewable energy source due to their potential for low-cost, lightweight, and large-area processabilty.[1] The most successful device structure for high performance PSCs is based on the bulk-heterojunction (BHJ) concept which involves a thin film blend of conjugated polymer as the electron donor and a fullerene derivative as the electron acceptor.[2] Among various types of polymers designed for PSCs, the donor−acceptor conjugated polymers based on the alternating electron-rich and electron-deficient units along the polymer backbone have been shown to be able to achieve high power convension efficiencies (PCEs).[2] The band gap and energy level of these conjugated polymers can be easily tuned by selecting different electron-rich and electron-deficient units. As a result, PCEs up to 7% have been demonstrated in these conjugated polymers through systematic optimizations of their absorption and open circuit voltage and relevant device parameters.[3]

Recently, benzodithiophene (BDT)-containing conjugated polymers have attracted great attention for their functions as electron donor for PSCs.[4] For instance, Yang et al. have synthesized the BDT-based copolymers with thiophene, benzothiadiazole, thieno[3,4-*b*]thiophene, and thieno[3,4-*b*]pyrazine units.[4] Among these polymers, poly(DBT-thieno[3,4-*b*]thiophene) showed the most promising photovoltaic performance (> 7%) due to the aromatic stabilization energy gained from forming the resonance quinoidal structure of the thieno[3,4-*b*]-thiophene units that significantly red-shifts the absorption of the polymers.[4b−d] These polymers possess a relatively high energy level for the highest occupied molecular orbital (HOMO) in the range of −5.2 and −4.6 eV. This contributes to lower open circuit voltage (V_{oc}) that can still be optimized to further improve the performance of the devices.

To achieve this goal, we have introduced 5-octylthieno[3,4-*c*]pyrrole-4,6-dione (TPD) as a new acceptor in the BDT-based copolymers. Because TPD can also gain some stabilization energy by forming a quinoidal thiophene−maleimide structure in its excited state, it is possible to afford a polymer with low energy band gap. The new polymer **PBDTTPD** was synthesized by the Stille coupling polymerization between 1,3-dibromo-5-octylthieno[3,4-*c*] pyrrole-4,6-dione and di(2-ethylhexyloxy)benzodithiophene distannane monomers. Both the conventional and inverted photovoltaic devices based on the blends of PBDTTPD and $PC_{71}BM$ were investigated. Under the AM 1.5G simulated solar illumination (100 mW/cm^2), maximum power conversion efficiencies (PCE) of > 4% could be achieved in both the conventional and inverted devices. Both devices exhibit large open-circuit voltage (V_{oc}) of up to 0.87 V, short-circuit current (J_{sc}) of up to 9.1 mA cm^{-2}, and external quantum efficiencies (EQE) exceeding 50% over the entire visible range (with a maxima of 65% at 540 nm). It is worthy to note that this polymer shows higher efficiency in the inverted device structure compared to the conventional device structure.

Scheme 1 shows the synthesis for monomers and polymers. Starting from benzo[1,2-*b*:4,5-*b*′]dithiophene-4,8-dione, the di(2-ethylhexyloxy) benzodithiophene distannane (**2**) was synthesized in three steps. The 1,3-dibromo-5-octylthieno[3,4-*c*]pyrrole-4,6-dione (**5**) was synthesized from thiophene-3,4-dicarboxylic anhydride, which was obtained from 3,4-dibromothiophene by adapting the methods reported in the literature.[5] Finally, the Stille polymerization of **2** and **5** was carried out using Pd-$(PPh_3)_4$ as catalyst in toluene/DMF to afford polymer PBDTTPD as a dark-blue solid. PBDTTPD shows good solubility in chlorinated solvents, such as chloroform, chlorobenzene, dichlorobenzene, and so forth. The number average molecular weight (M_n) of this polymer is measured to be 33 000 g/mol with a polydispersity (PDI) of 2.3 by gel permeation chromatography (GPC) with THF as the eluent. The results from differential scanning calorimetry (DSC) measurements show no obvious thermal transition between 20 and 300 °C.

---

(1) (a) Brabec, C. J.; Sariciftci, N. S.; Hummelen, C. J. *Adv. Funct. Mater.* **2001**, *11*, 15. (b) Krebs, F. C. *Sol. Energy Mater. Sol. Cells* **2009**, *93*, 394. (c) Dennler, G.; Scharber, M. C.; Brabec, C. J. *Adv. Mater.* **2009**, *21*, 1323.

(2) (a) Yu, G.; Gao, J.; Hummelen, J. C.; Wudl, F.; Heeger, A. J. *Science* **1995**, *270*, 1789. (b) Thompson, B. C.; Fréchet, J. M. J. *Angew. Chem., Int. Ed.* **2008**, *47*, 58. (c) Chen, J. W.; Cao, Y. *Acc. Chem. Res.* **2009**, *42*, 1709. (d) Cheng, Y. J.; Yang, S. H.; Hsu, C. S. *Chem. Rev.* **2009**, *109*, 5868.

(3) (a) Li, G.; Shrotriya, V.; Huang, J.; Yao, Y.; Moriarty, T.; Emery, K.; Yang, Y. *Nat. Mater.* **2005**, *4*, 864. (b) Peet, J.; Kim, J. Y.; Coates, N. E.; Ma, W. L.; Moses, D.; Heeger, A. J.; Bazan, G. C. *Nat. Mater.* **2007**, *6*, 497.

(4) (a) Hou, J. H.; Park, M. H.; Zhang, S. Q.; Yao, Y.; Chen, L. M.; Li, J. H.; Yang, Y. *Macromolecules* **2008**, *41*, 6012. (b) Liang, Y. Y.; Wu, Y.; Feng, D. Q.; Tsai, S. T.; Son, H. J.; Li, G.; Yu, L. P. *J. Am. Chem. Soc.* **2009**, *131*, 56. (c) Liang, Y. Y.; Feng, D. Q.; Wu, Y.; Tsai, S. T.; Li, G.; Ray, C.; Yu, L. P. *J. Am. Chem. Soc.* **2009**, *131*, 7792. (d) Hou, J. H.; Chen, H. Y.; Zhang, S. Q.; Chen, R. I.; Yang, Y.; Wu, Y.; Li, G. *J. Am. Chem. Soc.* **2009**, *131*, 15586.

(5) Nielsen, C. B.; Bjornholm, T. *Org. Lett.* **2004**, *6*, 3381.

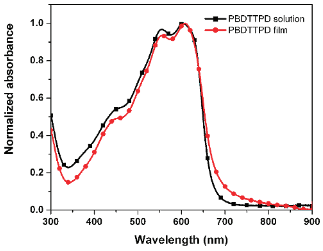

Figure 1. UV−vis spectra of PBDTTPD in $CHCl_3$ solution and film state.

Scheme 1. Synthetic Route for Polymer PBDTTPD

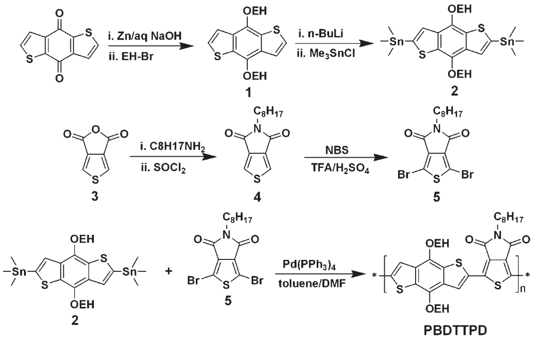

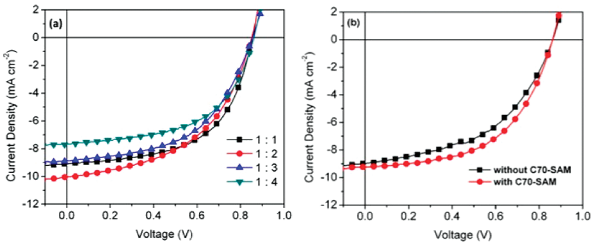

Figure 2. *J*−*V* curves of conventional devices (a) at various ratios of PBDTTI and $PC_{71}BM$ and inverted devices and (b) at a 1:2 ratio with and without the C_{70}-SAM layer under illumination of AM 1.5, 100 mW cm^{-2}.

Table 1. Performance of Photovoltaic Devices under the AM 1.5 Simulated Illumination (100 mW/cm^2)

ratio[a]	V_{oc} (V)	J_{sc} (mA cm^{-2})	FF	PCE (%)
1:1[b]	0.85 (±0.01)	8.7 (±0.2)	52.8 (±0.4)	3.9 (±0.1)
1:2[b]	0.84 (±0.02)	9.8 (±0.3)	49.5 (±0.6)	4.1 (±0.2)
1:3[b]	0.85 (±0.01)	8.5 (±0.2)	48.4 (±0.9)	3.5 (±0.2)
1:4[b]	0.86 (±0.01)	7.6 (±0.2)	48.6 (±1.1)	3.2 (±0.1)
1:2[c]	0.87 (±0.01)	9.0 (±0.1)	49.1 (±1.0)	3.8 (±0.1)
1:2[d]	0.87 (±0.01)	9.1 (±0.1)	53.8 (±1.1)	4.2 (±0.2)

[a] PBDTTPD and $PC_{71}BM$ ratio. [b] Conventional device. [c] Without C_{70}-SAM layer. [d] With C_{70}-SAM layer.

Figure 1a shows the absorption spectra of PBDTTPD in dilute chloroform solution and in the solid state. The spectra of PBDTTPD in solution and in thin film show a broad absorption that covers from 400 to 700 nm with a peak at 610 nm, which is probably due to the $\pi-\pi$ stacking of the polymer backbone. The absorption of the thin film is almost the same as that in solution which indicates that a certain degree of packing has already been formed even in the diluted solution. The optical band gap calculated from the absorption band edge of the PBDTTPD film is 1.82 eV. Electrochemical cyclic voltammetry was used to estimate the highest occupied molecular orbital (HOMO) and the lowest unoccupied molecular orbital (LUMO) energy levels of PBDTTPD. The HOMO and LUMO energy levels of PBDTTPD are −5.43 and −3.40 eV, respectively (Supporting Information, Figure S1). The band gap measured from CV (2.03 eV) is slightly larger than that obtained from the absorption spectrum-(1.82 eV), and similar phenomena have been observed previously with other PBDT-based polymers.[4a] The deeper HOMO level implies that the polymers could be more stable against oxidization, which will enhance the device stability. Since V_{oc} of the polymer BHJ devices is often proportional to the difference between the HOMO of the donor and the LUMO of the acceptor, a lower-lying HOMO of donor can result in higher V_{oc} and efficiency when blended with a fullerene derivative.

PSCs were first fabricated by using a conventional device structure: ITO/PEDOT:PSS/PBDTTPD:$PC_{71}BM$/LiF/Al (Figure 2 inset). $PC_{71}BM$ was chosen instead of $PC_{61}BM$ because of its stronger light absorption in the visible region. To understand the role of the ratio between polymer and $PC_{71}BM$ on the photovoltaic properties of PBDTTPD-based BHJ solar cells, devices with 1:1, 1:2, 1:3, and 1:4 of PBDTTPD:$PC_{71}BM$ weight ratios were fabricated and tested. The *J*−*V* curves of the resulting four devices are shown in Figure 2a. The average photovoltaic performance is summarized in Table 1. A maximum PCE of 4.1%, an open-circuit voltage (V_{oc}) of 0.84 V, a short-circuit current (J_{sc}) of 9.8 mA cm^{-2}, and a fill factor (FF) of 49.5% could be achieved based on a PBDTTPD:$PC_{71}BM$ ratio of 1:2 with a thin active-layer thickness of 90 nm (Figure 2, Table 1). The J_{sc} of the device first increases from 8.7 mA cm^{-2} at a PBDTTPD:$PC_{71}BM$ blend ratio of 1:1 to 9.8 mA cm^{-2} at 1:2 and then decreases to 7.6 mA cm^{-2} at 1:4, which is typical for BHJ photovoltaic cells due to less and less light absorbing materials in the active layer. The V_{oc} shows a similar value of ∼0.85 V at all ratios. FF decreases with the increase of $PC_{71}BM$ content. As expected, V_{oc} as high as 0.85 V could be achieved. It is consistent with the observed low HOMO level of PBDTTPD (−5.43 eV) since V_{oc} is the difference between the HOMO energy level of the polymer and the LUMO energy level of $PC_{71}BM$ (−4.30 eV).

The morphology of thin film is also very important for the performance of polymer/fullerene BHJ solar cells. The morphology of pristine PBDTTPD film and PBDTTPD blended with $PC_{71}BM$ (1:2) film were investigated using tapping-mode atomic force microscopy (AFM). Figure 3 shows the AFM images of pristine PBDTTPD and PBDTTPD/$PC_{71}BM$ blended films. The images show a smooth surface and small phase segregration features in both the pristine and the blended films indicating good film formation of the materials.

In the conventional device configuration, the conducting polymer, PEDOT:PSS, and a low-work-function metal are often used as anode and cathode contact, respectively. However, the acidic nature of PEDOT:PSS tends to etch ITO results in unstable contact, and the low work function metals such as calcium and aluminum are very sensitive to the environment which will significantly

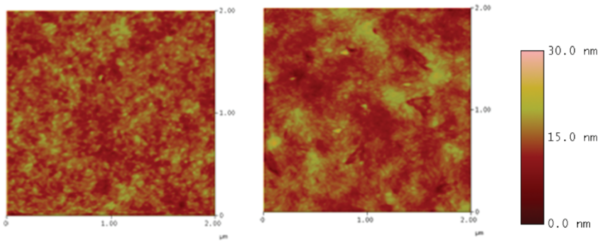

Figure 3. AFM topography images of pristine PBDTTPD (a) and PBDTTPD:$PC_{71}BM$ (1:2) (b) films. Height scale: 30 nm.

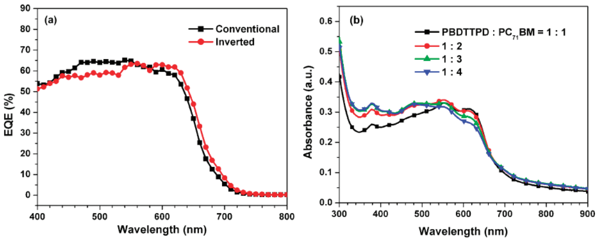

Figure 4. External quantum efficiency of conventional and inverted devices (a) and the absorption spectra (b) of PBDTTPD:$PC_{71}BM$ thin films with various ratios.

deterioate the device performance.[6] To alleviate these problems, inverted device configuration has been employed by modifying ITO with a thin layer of Cs_2CO_3, TiO_x, or ZnO for functioning as an efficient electron collection cathode and a stable metal (such as Ag or Au) as anode to collect holes.[7] Although this device structure is promising, very few conjugated polymers have been successfully incorporated into an inverted device to show good performance. Among them, P3HT is still the top performer. To test the suitability of using PBDTTPD in an inverted device structure, we have used the following two configurations: ITO/ZnO/PBDTTPD:$PC_{71}BM$ (1:2)/PEDOT:PSS/Ag and ITO/ZnO/C_{70}-SAM/PBDTTPD:$PC_{71}BM$ (1:2)/PEDOT:PSS/Ag. The C_{70}-SAM is based on a carboxylic acid functionalized C_{70} molecule to modify the ZnO surface (see Supporting Information for chemical strucutre) which has been proved to be very effective in improving the inverted device performance because it acts as both a nice interface for exciton separation and electron selection.[8] The $J-V$ characteristics of two inverted devices are shown in Figure 3b. Under the AM 1.5 simulated solar illumination (100 mW/cm^2), the C_{70}-SAM modified device shows a high PCE of 4.2% compared to 3.8% from the unmodified device. A V_{oc} of ~0.87 V was observed for both devices. Similar J_{sc} values of 9.0 and 9.1 mA cm^{-2} and fill factors (FF) of 49.1% and 53.8% were achieved for unmodified and C_{70}-SAM modified devices, respectively (see Supporting Information for the data with different ratios). The higher FF shows the advantage of the SAM modification. To the best of our knowledge, these results are among the highest reported for donor−acceptor type polymers with better performance in the inverted device structure than in the conventional structure.

The EQE is used to evaluate the photoresponse of the fabricated solar cells. Both the EQEs of the conventional and inverted devices with PBDTTPD:$PC_{71}BM$ blend (at a ratio of 1:2) as active layer were measured. The EQE curves are shown in Figure 4a. Both devices show similar and rather efficient photoconversion efficiency between 400 and 700 nm with the EQE value as high as 65.2%. To further improve the accuracy of measurements, the J_{sc} values were also calculated by integrating the EQE data compared with an AM1.5 reference spectrum. The calculated J_{sc} values were 10.0 and 10.1 mA/cm^2 for the conventional and inverted devices, respectively. These values are close to those obtained from the $J-V$ measurements. The absorption curves of PBDTTPD:$PC_{71}BM$ blend films at different ratios are shown in Figure 4b.

Significant increases in absorption could be observed in the range between 300 and 700 nm after blending with $PC_{71}BM$. By increasing the content of $PC_{71}BM$, the absorption between 350 and 550 nm becomes stronger and the absorption from PBDTTPD starts to decrease, which is consistent with the observed device efficiency (Table 1). Since mobility of polymer is also an important parameter that can affect the performance of solar cells, hole mobility of PBDTTPD is measured in a field-effect transistor with a bottom-gate, top-contact device configuration built on an n-doped silicon wafer. The hole mobility of PBDTTPD extracted from the saturation regime is $\sim 4.6 \times 10^{-5}$ cm^2 V^{-1} s^{-1} which is similar to other low band gap conjugated polymers.[9]

In conclusion, bulk heterojunction solar cells based on a novel low band gap polymer, PBDTTPD, were investigated. In the conventional device structures, a power conversion efficiency of 4.1% could be achieved from the thin film blend of PBDTTPD:$PC_{71}BM$ (1:2) with a current density of 9.8 mA cm^{-2}, V_{oc} of 0.84 V, and FF of ~50%. The high V_{oc} (0.87 V) is the result of the lower HOMO level of the polymer. In addition, inverted devices with PBDTTPD:$PC_{71}BM$ (1:2) as active layer were also investigated.

Acknowledgment. The authors are grateful for the support of the National Science Foundation's STC program under DMR-0120967, the Department of Energy "Future Generation Photovoltaic Devices and Process" program under DE-FC36-08GO18024/A000, the AFOSR's "Interface Engineering" Program under FA9550-09-1-0426, and the Office of Naval Research under N00014−08−1−1129. A. K. Y. Jen thanks the Boeing-Johnson Foundation for the financial support.

Supporting Information Available: Experiment details, the fabrication and characterization of the devices, measurements, and instruments. This material is available free of charge via the Internet at http://pubs.acs.org.

---

(6) Li, G.; Chu, C. W.; Shrotriya, V.; Huang, J.; Yang, Y. *Appl. Phys. Lett.* **2006**, *88*, 253503.

(7) (a) Hau, S. K.; Yip, H. L.; Baek, N. S.; Zou, J. Y.; O'Malley, K.; Jen, A. K. Y. *Appl. Phys. Lett.* **2008**, *92*, 253301. (b) Chen, L. M.; Hong, Z. R.; Li, G.; Yang, Y. *Adv. Mater.* **2009**, *21*, 1434. (c) Kim, C. S.; Lee, S.; Gomez, E. D.; Kim, J.; Loo, Y. L. *Appl. Phys. Lett.* **2009**, *94*, 113302. (d) Steim, R.; Choulis, S. A.; Schilinsky, P.; Brabec, C. J. *Appl. Phys. Lett.* **2008**, *92*, 093303.

(8) Hau, S. K.; Yip, H. L.; Acton, O.; Beak, N. S.; Ma, H.; Jen, A. K. Y. *J. Mater. Chem.* **2008**, *18*, 5113.

(9) Qin, R.; Li, W.; Li, C.; Du, C.; Veit, C.; Schleiermacher, H. S.; Andersson, M.; Bo, Z.; Liu, Z.; Inganäs, O.; Wuerfel, U.; Zhang, F. *J. Am. Chem. Soc.* **2009**, *131*, 14612.